Shell model study of the neutron-rich nuclei around $N=28$

J. Retamosa,[1] E. Caurier,[1] F. Nowacki,[2] and A. Poves[3]
[1]*CRN IN2P3-CNRS/Université Louis Pasteur, Boîte Postale 28, F-67037 Strasbourg-Cedex, France*
[2]*GANIL IN2P3-CNRS, Boîte Postale 5027, F-14021 Caen-Cedex, France*
[3]*Departamento de Física Teórica C-XI, Universidad Autónoma de Madrid, E-28049 Madrid, Spain*
(Received 6 August 1996)

We describe the properties of the neutron-rich nuclei around $N=28$ in the shell mode framework. The valence space includes the sd shell for protons and the pf shell for neutrons without any restriction. Good agreement is found with the available experimental data. The $N=28$ shell closure persists, even if eroded by the large neutron excess. The calculations predict that ^{40}S and ^{42}S are deformed with $\beta=0.29$ and $\beta=0.32$ respectively. [S0556-2813(97)00802-9]

PACS number(s): 21.60.Cs, 21.10.Tg, 27.30.+t, 27.40.+z

I. INTRODUCTION

The exploration of the behavior of the nucleus under extreme conditions; high spin, vicinity of the drip lines, finite temperature, etc., is a major source of new insights into nuclear structure. One of the most important questions raised by the study of the drip lines is whether the basic shell order evolves with the neutron (proton) excess. An example of this problem is given by the $N=20$ very neutron rich nuclei where the strong anomalies detected [1–4] were explained as a collapse of the standard $N=20$ shell closure. Extended shell model calculations [5–7] showed that the inversion of the spherical closed-shell configurations and the $2p$-$2h$ collective intruders could account for the large binding energies and half-lives, unexpected ground-state spins, and high level densities at low excitation energies. Also, mean-field calculations using the Skyrme interaction predicted a sharp transition from spherical to prolate shapes [8].

Recently, there has been an increase of interest in the $N=28$ isotones far from the stability, motivated by; (i) the possible existence of anomalies in the shell closures, as already found in $N=20$ and (ii) the unusual ^{48}Ca/^{46}Ca abundance ratio measured in the solar system or the Ca-Ti-Cr anomalies observed in some meteoritic inclusions.

Sorlin *et al.* [9] undertook the study of the β decay and β-delayed neutron emission probability for ^{44}S and $^{45-47}$Cl. Their measured half-lives were found much shorter than those predicted by Tamm-Dancoff approximation [10] or quasiparticle random-phase approximation [11] calculations. These discrepancies were attributed to unexpected shape transitions in the region. Mass formulas such as the finite-range liquid drop [12], the finite-range droplet [13], or the extended Thomas-Fermi with shell corrections expressions [14] predict the existence of shape coexistence around ^{44}S. In any case the energy surfaces are very soft with close lying minima corresponding to different deformations.

Similar conclusions have been drawn by Werner *et al.* [15]. Relativistic mean-field calculations and nonrelativistic ones using the Skyrme forces produce very flat energy surfaces for the sulphur isotopes, with several minima separated by energy barriers of just a few hundred KeV. In this situation it seems necessary to go beyond the mean-field approximation using, for instance, the generator coordinate method.

In this paper we discuss all the neutron-rich nuclei with $N\geqslant 20$ and $14\leqslant Z\leqslant 20$ in the shell model framework. This is, to some extent, complementary to the other methods mentioned above and can give new information on the structure of these nuclei. The paper is organized as follows. Section II gives a brief description of the model, discussing the choice of the valence space, the effective interaction and the Coulomb corrections. Section III compares our results with the experimental data. In Sec. IV we examine the behavior of the $N=28$ shell closure far from stability. Section V deals with deformation in heavy S isotopes.

II. THE MODEL

A. The valence space

The valence space consists of the full sd shell for Z-8 protons and the full pf shell for N-20 neutrons. Although the calculations reach very large dimensionalities, they can be performed without truncations in all cases. We do not include the intruder states that could be formed by exciting particles from the sd to the pf shell. This category of states that appear at low excitation energy around ^{40}Ca, should be less important near $N=28$. The reason is twofold; sd protons get more and more bound with increasing neutron excess then unfavoring proton intruders and the configurations with neutron intruders do not gain much energy compared with the single particle energy gap. This result is in agreement with the observed spectra. The existence of many collective low lying states near $N=Z=20$ contrast with their absence for $N\simeq 28$, $Z>20$.

B. The interaction

The construction of the effective Hamiltonian is critical in any shell model description. It is well known that the saturation properties of the realistic interactions must be corrected phenomenologically in order to have a good description of the nuclear structure [16]. Unfortunately, the experimental data for the very neutron-rich nuclei with $14\leqslant Z\leqslant 18$ are scarce. Although masses are known over a relatively wide region, at $N=28$ they have only been measured for nuclei with $Z\geqslant 19$. As an example the masses of the S isotopes are only known up to $N=26$ and the half-life

values are restricted to ^{44}S, $^{45-47}$Cl, and ^{43}P. The level schemes of Ar and Cl with $20 \leqslant N \leqslant 23$ are partly established. The situation is clearly better for the K isotopes where the evolution of the $3/2^+,1/2^+$ doublet with the neutron number is known up to $N=28$ [17].

Our starting interaction has three parts. The USD interaction of Wildenthal [18] is used for the particles lying in the sd shell. A modified version of the Kuo-Brown interaction, denoted KB′ in Ref. [19], gives the two body matrix elements for the pf shell particles. This interaction is better suited to this valence space than the KB3 interaction that has been used in conventional pf shell calculations [24]. Furthermore, when used in the lower part of the pf shell it also gives good spectroscopic results. Finally, the cross-shell interaction is the G matrix of Lee, Kahanna, and Scott (LKS) [20]. This is the part of the interaction that we have proceeded to modify phenomenologically. The data used in the fit are (i) The natural parity states of nuclei with few pf particles and sd holes, (ii) The evolution of the $3/2^+,1/2^+$ doublet along the K isotopes, (iii) The position of the $5/2^+$ states in ^{47}K.

The experimental data quoted above are not sufficient to fix all the monopole parameters. They essentially settle the interaction among neutrons in the $1f_{7/2}$ and $2p_{3/2}$ orbits with the sd protons. On the contrary, the interaction with $1f_{5/2}$ and $2p_{1/2}$ particles is not well determined. In our choice of the final interaction ^{41}Ca and ^{35}Si have very similar single neutron spectra as suggested by the monopole systematics [21]. There exists, however, other possible choices of this part of the interaction that induce important modifications in the structure of heavy silicons and to a minor extent in that of the heavy sulphurs.

The two-body matrix elements incorporate a tiny mass dependence and are written as:

$$V=\frac{\omega(A)}{\omega(A_0)}V_0=\frac{\langle r^2(A_0)\rangle}{\langle r^2(A)\rangle}V_0, \tag{1}$$

where $A_0=40$ and $\hbar\omega_0=11$ MeV are used to calculate the LKS G matrix. Instead of the usual law $\langle r^2\rangle = r_0 A^{1/3}$ fm, we borrow from Ref. [22] a modified expression, which is better fitted to large mass regions,

$$\langle r^2\rangle = r_0\left\{A\left[1-\zeta\left(\frac{N-Z}{A}\right)^{1/2}\right]\right\}^{1/3}. \tag{2}$$

Then the following expression for the two-body matrix elements can be deduced:

$$V=\left\{\left(\frac{A_0}{A}\right)\left[1-\zeta\left(\frac{N-Z}{A}\right)^{1/2}\right]\right\}^{1/3}V_0 \tag{3}$$

with $\zeta=0.42$ and $A_0=40$.

C. Coulomb energies

The absolute energies predicted with the above interaction are relative to a ^{16}O core and do not include the Coulomb energy of the protons. Thus, to compare our predictions with experiment, they must be corrected with the following prescription:

TABLE I. 2_1^+ excitation energy (in MeV). For numbers with an asterisk see the note added on proofs.

	N	22	24	26	28	30
Cr	th	0.869	0.742	0.793	1.621	0.877
	exp		0.751	0.783	1.434	0.835
Ti	th	1.209	0.869	1.003	1.755	1.103
	exp	1.083	0.889	0.983	1.555	1.047
Ca	th	1.534	1.409	1.338	3.947	1.110
	exp	1.524	1.157	1.347	3.832	1.030
Ar	th	1.368	1.249	1.182	1.655	1.219
	exp	1.461	1.208	1.144*	1.554*	
S	th	1.209	1.047	1.073	1.645	1.272
	exp	1.286*	0.891*	0.890*		
Si	th	1.900	1.670	1.652	2.558	1.461
	exp					

$$E_i(N,Z)=E_0+E_c(N,Z)+E_i^{\mathrm{SM}}(N,Z), \tag{4}$$

where E_0 is the inert core energy (127.62 MeV), $E_c(N,Z)$ is the Coulomb energy relative to the core, and E_i^{SM} is the nuclear energy obtained with our interaction. The E_c energy, which is assumed to depend only on N and Z, has been calculated with the Antony and Pape formula [23]

$$E_c(A,Z) = \begin{cases} E_c(A,Z-1)+1.44(Z-1/2)/A^{1/3}-1.02 & Z>Z_s \\ E_c(A,Z+1)-1.44(Z+1/2)/A^{1/3}+1.02 & Z<Z_s, \end{cases} \tag{5}$$

where $Z_s=A/2$ or $(A+1)/2$ and the Coulomb correction $E_c(Z_s)$ along the stability line is given by

$$E_c(Z_s)=\begin{cases} 0.162Z^2+0.95Z-18.25 & Z\leqslant 20 \\ 0.125Z^2+2.35Z-31.53 & Z>20, \end{cases} \tag{6}$$

which agrees with the Chung-Wildenthal coulomb correction [6] when $Z_s\leqslant 20$ and with that of Ref. [24] for $Z_s>20$.

III. RESULTS AND DISCUSSION

A. Comparison with the data

In this section we compare the theoretical predictions with the experimental data. The shell model matrices are dealt with by the code ANTOINE [25], a very fast and efficient implementation of the Lanczos algorithm . The USD predictions for the sd-shell nuclei have been largely reported [18]. However, we shall include sd nuclei in the S_{2N} plots to illustrate the continuity of the shell model description across the $N=20$ magic number.

Table I contains the predicted and experimental energies of the 2^+ states, which are found to be in excellent agreement. The interaction, adjusted to reproduce the behavior of

TABLE II. Energy difference between the $3/2^+_1$ and $1/2^+_1$ states in K, Cl, and P.

	N	20	22	24	26	28	30
K	th	2.73	0.96	0.67	0.28	−0.38	0.19
$E(1/2)-E(3/2)$	exp	2.52	0.98	0.56	0.47	−0.36	
Cl	th	1.82	0.71	0.06	−0.21	−0.05	−0.06
$E(1/2)-E(3/2)$	exp	1.73	0.40				
P	th	2.61	1.32	0.68	0.32	0.06	0.38
$E(3/2)-E(1/2)$	exp						

the $3/2^+$, $1/2^+$ levels along the odd-A K isotopes, predicts for the doublet a similar behavior in the neutron rich Cl and P isotopes (see Table II). The crossing of these two levels is due to the gradual degeneracy of the $2s_{1/2}$ and $1d_{3/2}$ orbitals as the occupation of the $1f_{7/2}$ shell increases. In the P isotopes, the $1d_{5/2}$ orbit is nearly closed, consequently the evolution of the doublet gives us an estimate of the relative position of the two orbitals. As we shall comment later, their relative position is the determining factor for the development of deformation in the heavy sulphurs.

The spectroscopic information on the nuclei with $Z<20$, $N>20$ is limited to some K, Ar, and Cl isotopes [28]. Figures 1 to 8 show the theoretical and experimental spectra for the cases —$^{40-42}$K, $^{39-42}$Ar, and ^{38}Cl— for which the energy levels are known. Yet, there are still many uncertainties in the measured level schemes, specially the spin assignments. The theory-experiment agreement is perfect for $^{40-41}$K and ^{40}Ar. The few states without theoretical counterpart are most probably sd intruders. For the other nuclei the concordance is also quite good.

In addition to these spectra, half-lives are known for several Ar and S isotopes, as well as for ^{44}Cl and ^{43}P [9]. We shall only consider the decays of the even-even nuclei. They are dominated by allowed Gamow-Teller transitions. The ground states of the father nuclei were calculated in our $0\hbar\omega$ space and the Gamow-Teller sum rule state was determined in a larger space that includes all the $1p-1h$ states in order to recover the $3(N-Z)$ sum rule. The strength functions were obtained by the Whitehead method [26]. The phase space factors of Wilkinson [27] were used to compute the half-lives. The theory-experiment agreement is very satisfactory as it can be seen in Table III, which contains the total strengths and half-lives. The calculated half-life of ^{44}S is very sensitive to the Q_β. We have used the theoretical value; if we had taken the extrapolated number given in the

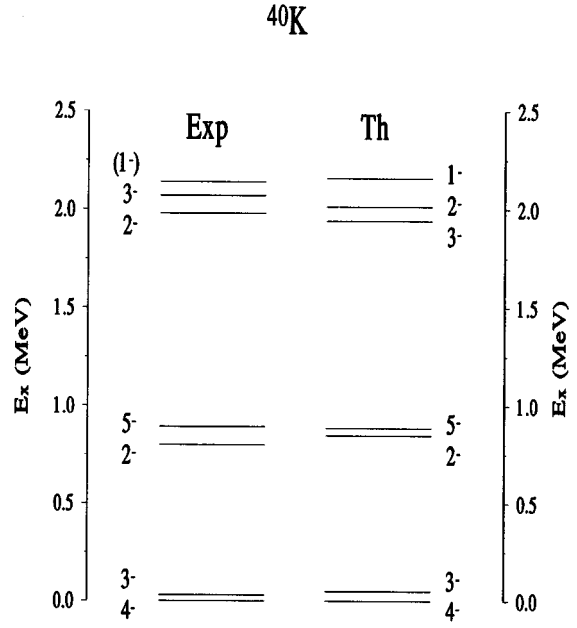

FIG. 1. Theoretical and experimental natural parity states for ^{40}K.

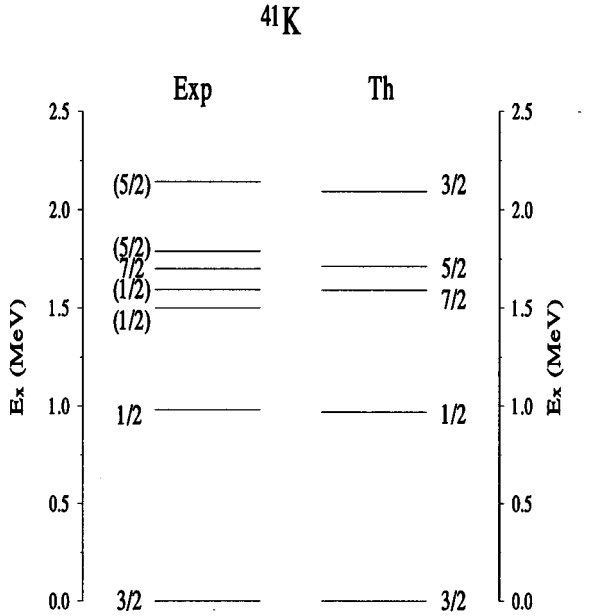

FIG. 2. Same as Fig. 1 for ^{41}K.

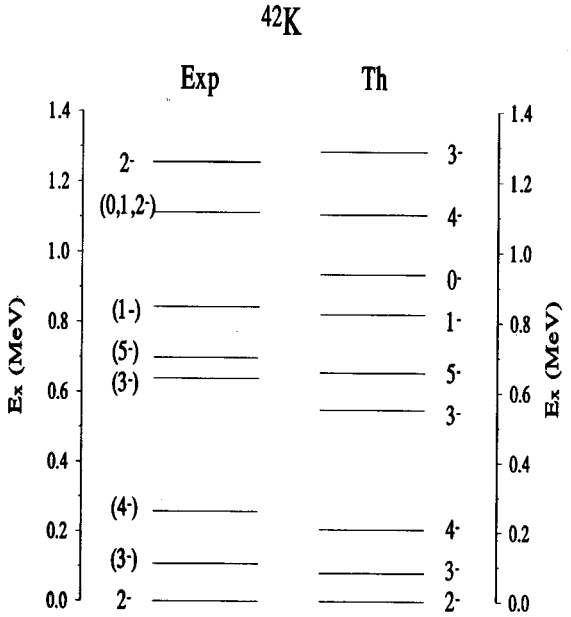

FIG. 3. Same as Fig. 1 for ^{42}K.

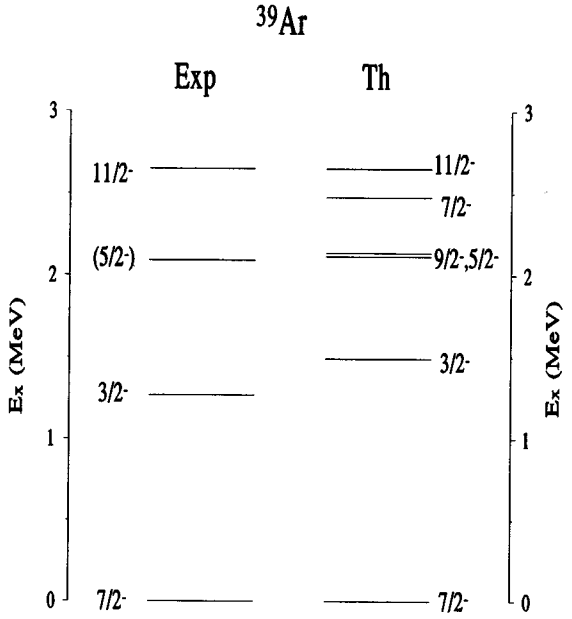

FIG. 4. Same as Fig. 1 for ^{39}Ar.

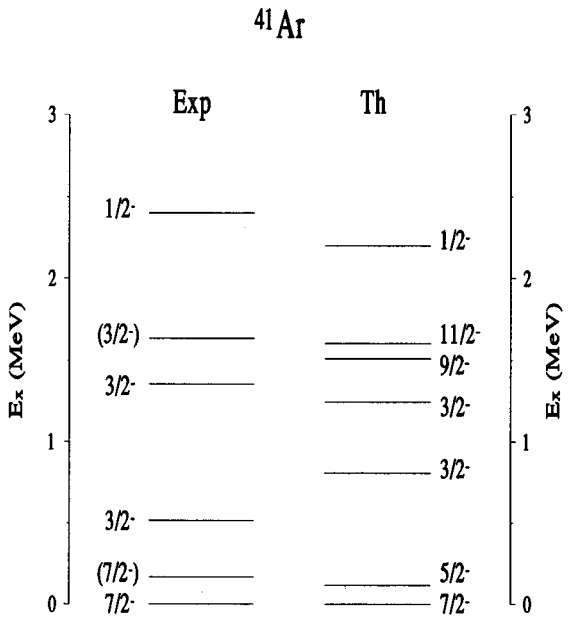

FIG. 6. Same as Fig. 1 for ^{41}Ar.

Audi and Wapstra compilation [29], the half-life would have increased to 197 ms.

The two neutron separation energies S_{2N} are known over a large region, unfortunately, for most Z values they do not reach $N=28$. The agreement with the experimental results is good as it can be seen in Figures 9 to 15. However, the discrepancies with the extrapolated masses [29] are important.

B. Does the $N=28$ shell gap persist with large neutron excess?

To answer this question we analyze our predictions for the S_{2N}, the excitation energies of the first 2^+ states, and the occupation numbers. Structural changes, such as spherical to deformed shape transitions, should show up in the behavior of these quantities as a function of the neutron number.

The S_{2N} variations around $N=28$ have some common features for different Z values. In three cases, Ca, K, and Si, a sharp decrease of S_{2N} is observed at $N=28$. For the other isotopes, there are not sharp changes in the slopes, but S_{2N} still decreases. These results are consistent with a shell closure. Such conclusion is opposite to that coming from the mass systematic extrapolations, which lead to almost constant S_{2N} around $N=28$, interpreted as a signature of a new region of deformation.

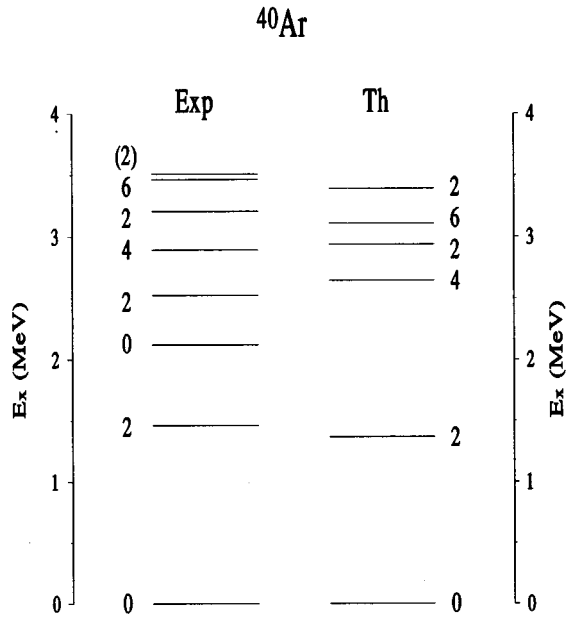

FIG. 5. Same as Fig. 1 for ^{40}Ar.

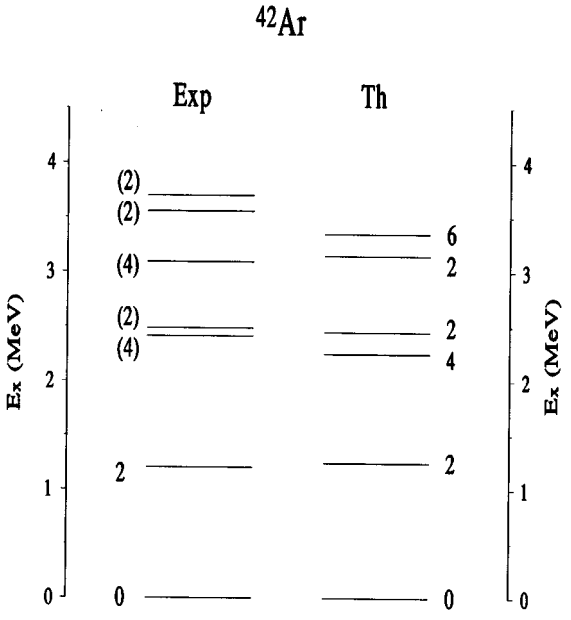

FIG. 7. Same as Fig. 1 for ^{42}Ar.

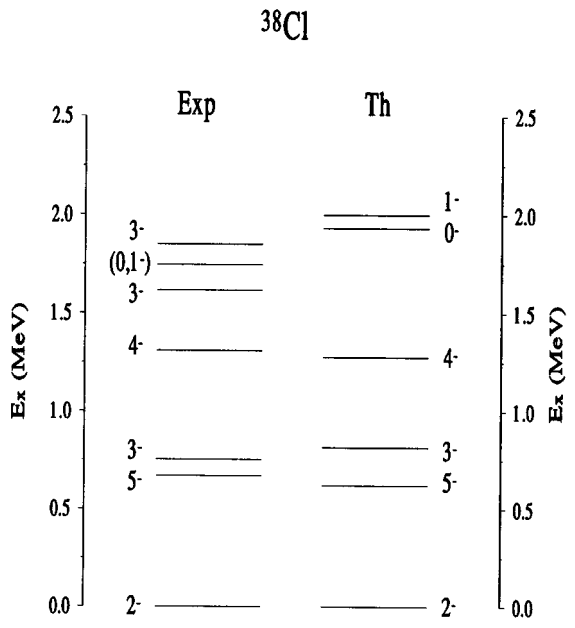

FIG. 8. Same as Fig. 1 for ^{38}Cl.

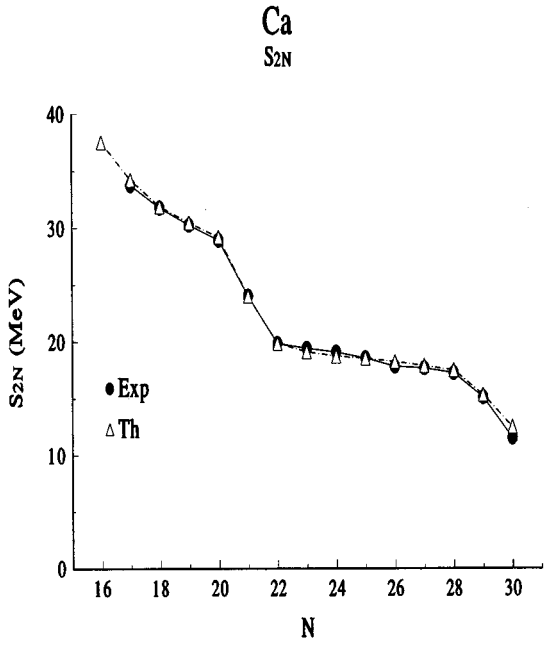

FIG. 9. S_{2n} energies for the Ca isotopes.

Figure 16 shows the evolution of the 2^+ energy for the Ca and Si isotopes. The large energy increase of the 2^+ state for the four nuclei ^{40}Ca, ^{48}Ca, ^{34}S, and ^{42}Si is a characteristic of doubly magic nuclei. Notice, however, that the effect is smaller for the exotic ^{42}Si. A similar evidence comes from the $1f_{7/2}$ occupation numbers along $N=28$. Those, shown in Fig. 17, reveal an increase of the $1f_{7/2}$ occupation at $Z=20$ and $Z=14$, which is again smaller in ^{42}Si.

The 2^+ excitation energies of the isotopes of Ar and S, around $N=28$, are presented in Fig. 18 and compared with the corresponding energies of nuclei much closer to the stability at those neutron numbers (Ti, Cr). There is an upward shift of the excitation energies at $N=28$ that is a little smaller in Ar and S. The behavior is seen to be very similar close and far off stability, thus indicating that the $N=28$ closure stands in the very neutron-rich region.

From the analysis of these three sets of results, S_{2N}, $E_x(2^+)$, and the occupation numbers we can conclude that the $(1f_{7/2})^8$ neutron configuration at $N=28$, although somewhat eroded by the large neutron excess, is still dominant and that ^{42}Si is a new doubly magic nucleus. Therefore, the vanishing of the shell closure far from stability that happens at $N=20$, does not seem to occur at $N=28$.

TABLE III. Total Gamow-Teller strength, theoretical and experimental half-lives for the even-even Ar and S isotopes.

	GT^-	$T^{th}_{1/2}$	$T^{exp}_{1/2}$
^{44}Ar	22.85	4.70 m	11.87 m
^{46}Ar	28.84	6.94 s	8.4 s
^{38}S	16.78	174.4 m	170.3 m
^{40}S	22.87	6.67 s	8.8 s
^{42}S	28.89	389 ms	560 ms
^{44}S	34.93	54 ms	123 ms

C. The deformed nuclei ^{40}S and ^{42}S

Our calculations show the existence of low lying 2^+ states for the Ar and S isotopes with $22 \leqslant N \leqslant 26$. However, only the S isotopes have large (and negative) spectroscopic quadrupole moments and enhanced $E2$ transitions (see Figs. 19 and 20). ^{42}Ar and ^{44}Ar have reasonably large $BE2$'s but very small spectroscopic quadrupole moments.

The lowest 2^+ energies correspond to ^{40}S and ^{42}S. Their spectroscopic quadrupole moments are -17.1 and -19.2 e^2fm^2 respectively. Assuming that the Bohr-Mottelson formula for the intrinsic quadrupole moment is applicable, we

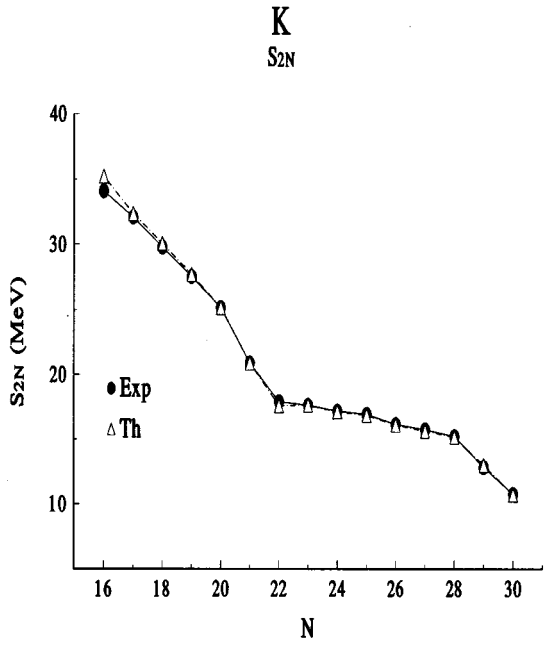

FIG. 10. S_{2n} energies for the K isotopes.

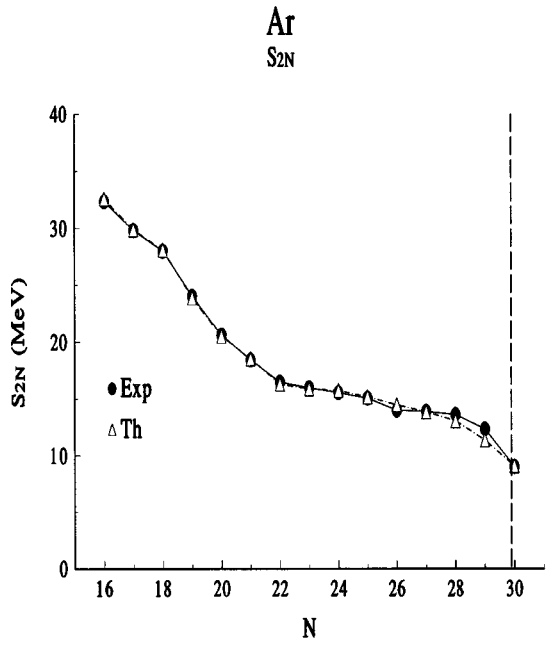

FIG. 11. S_{2n} energies for the Ar isotopes. The experimental points beyond the vertical line are not measured quantities but numbers from Audi and Wapstra's extrapolations.

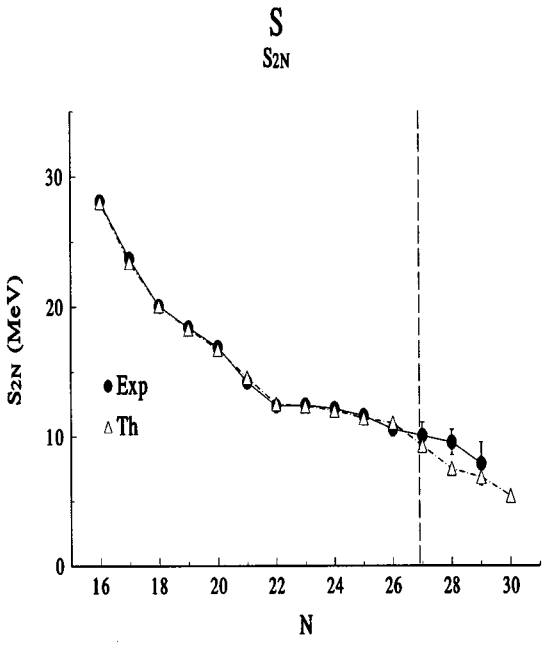

FIG. 13. S_{2n} energies for the S isotopes. See caption to Fig. 11.

get $Q_0=59.8\ e^2\mathrm{fm}^2$ for ^{40}S and $Q_0=67.2\ e^2\mathrm{fm}^2$ for ^{42}S, corresponding to deformation parameters $\beta\simeq 0.29$ and $\beta\simeq 0.32$. Our results are consistent with the relativistic mean-field calculations of Werner *et al.*, which predict $\beta\simeq 0.25$ for ^{42}S. Their nonrelativistic calculations point to a more complicated situation with nearly degenerate prolate ($\beta\simeq 0.25$) and oblate ($\beta\simeq -0.24$) solutions. The only indication of coexistence in our results is provided by the presence of a very low (1.51 MeV) second 0^+ state in ^{44}S.

The values of the $E2$ reduced transition probabilities are 77.9 $e^2\mathrm{fm}^4$ ($A=40$) and 93.0 $e^2\mathrm{fm}^4$ ($A=42$). We compare the quadrupole moments of ^{42}S and other nuclei near $N=28$ in Fig. 14. The value for ^{42}S is about 2/3 of that predicted for ^{48}Cr leading to very similar deformation parameters $\beta=0.32$ and $\beta=0.30$. In addition, the yrast levels of ^{42}S follow the rotational law $J(J+1)$ up to $J=6$.

It is also important to notice that, although a truncated $1f_{7/2}\,2p_{3/2}$ valence space for the neutrons, contains the basic degrees of freedom for the description of deformed nuclei in this region, it enhances either the rotational behavior or the

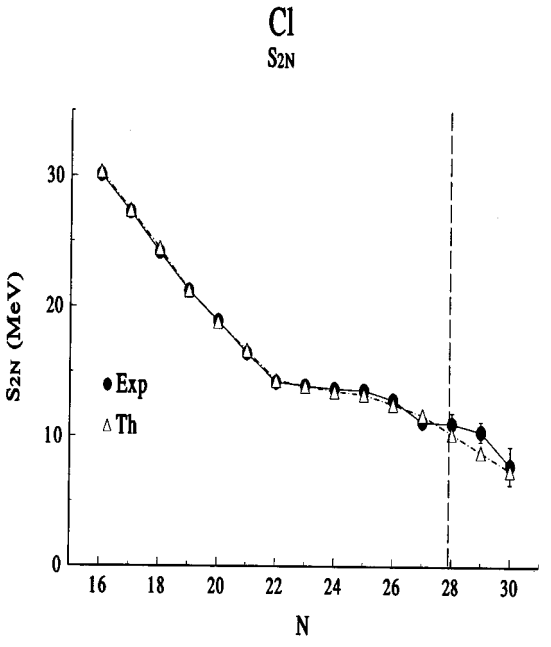

FIG. 12. S_{2n} energies for the Cl isotopes. See caption to Fig. 11.

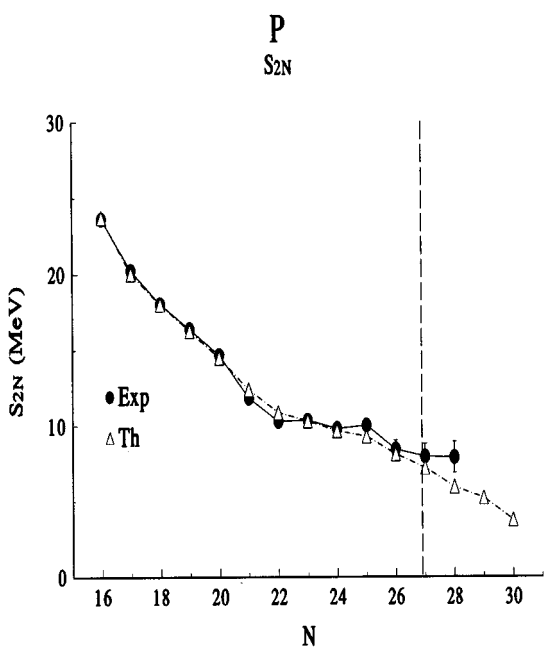

FIG. 14. S_{2n} energies for the P isotopes. See caption to Fig. 11.

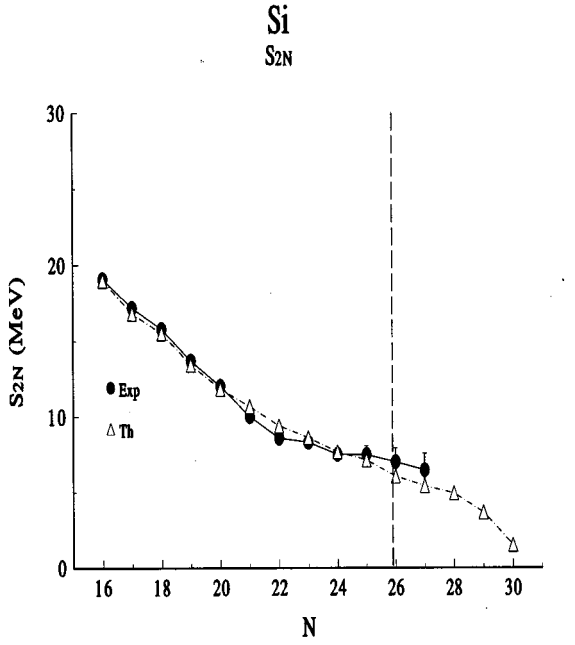

FIG. 15. S_{2n} energies for the Si isotopes. See caption to Fig. 11.

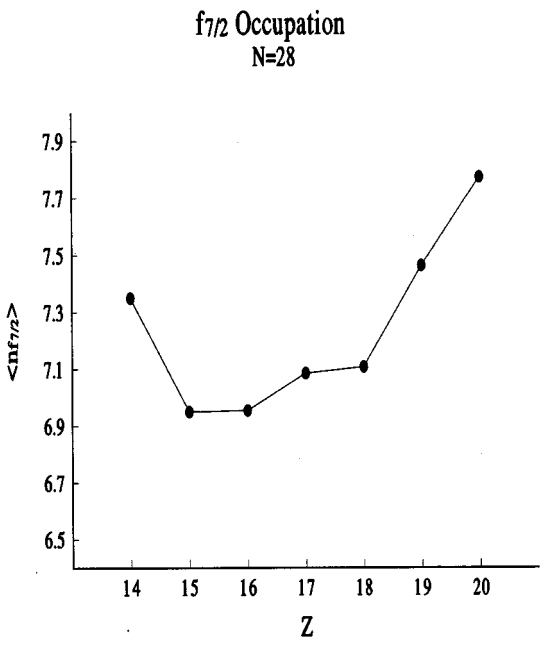

FIG. 17. $f_{7/2}$ occupation numbers.

closed shell features, depending on the basic configurations that are involved. As an example let us consider the evolution of the 2^+ excitation energies of the S isotopes. In the truncated space the energy of the 2^+ state in $N=26$ goes down to 0.88 MeV while in $N=28$ it goes up to 1.78 MeV.

In order to explain the onset of deformation we shall explore which are the configurations responsible for the quadrupole coherence in our space. It is well known that the SU(3) symmetry is broken by the strong $\vec{l}\cdot\vec{s}$ coupling in the pf shell. Yet, it has been recently shown [30] that the subspaces of a major shell spanned by $\Delta j=2$ orbits develop an approximate SU(3) symmetry, named quasi-SU(3). For instance the $1f_{7/2}\,2p_{3/2}$ valence space is enough to explain the collective behavior of nuclei in the pf shell. In this space the maximal quadrupole collectivity is obtained for configurations with four protons and four neutrons. In our case, the basic neutron degrees of freedom are contained in this space, but protons are confined in the sd shell. For the nuclei we are interested in, the orbit $1d_{5/2}$ is essentially closed and only the $1d_{3/2}$ and the $2s_{1/2}$ can be considered active. In this situation neither SU(3) nor quasi-SU(3) can develop.

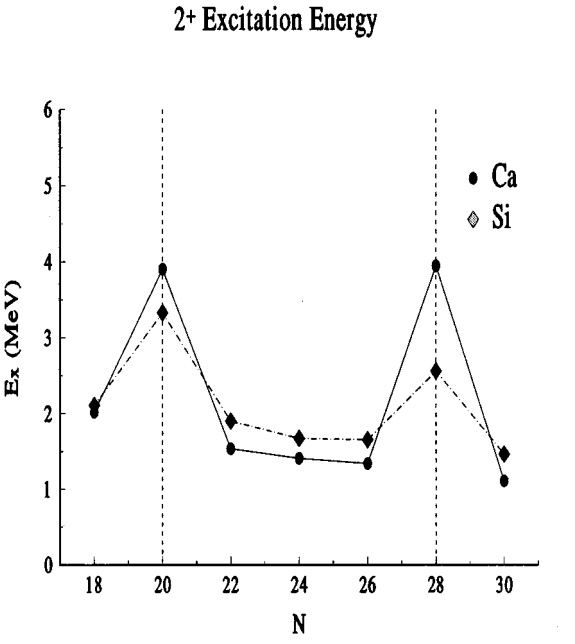

FIG. 16. 2^+ excitation energies for the Ca and Si isotopes.

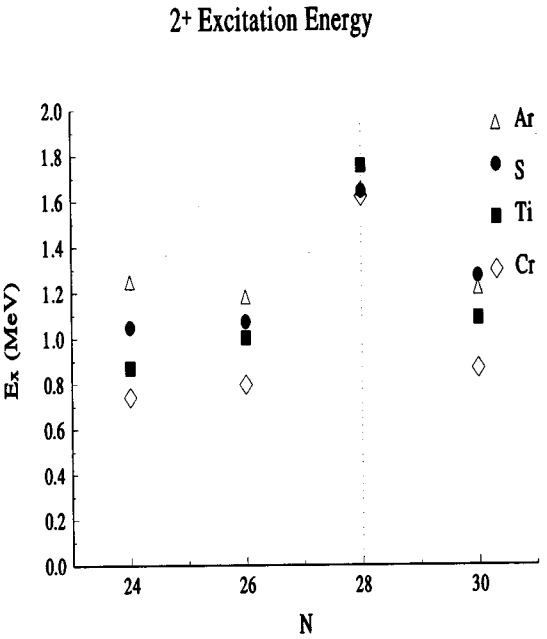

FIG. 18. 2^+ excitation energies for the Ar, S, Ti, and Cr isotopes.

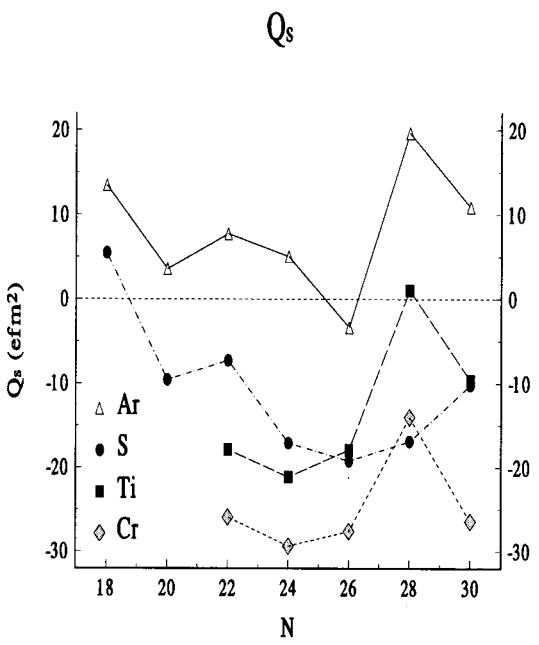

FIG. 19. Spectroscopic quadrupole moments for the Cr, Ti, Ar, and S isotopes.

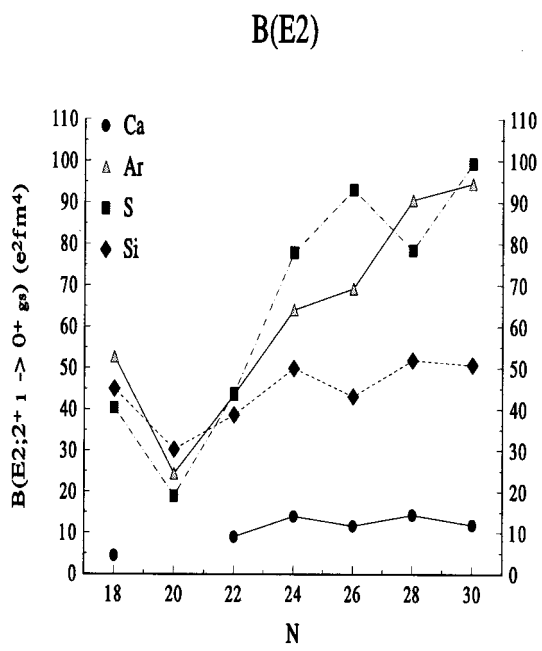

FIG. 20. $BE2$ for Ca, Ar, S, and Si isotopes.

However, one must look more carefully at the behavior of these two orbits. As far as the neutrons are filling the sd shell, both orbits remain well separated. For instance, the excitation energy of the $3/2_1$ level in ^{29}P and ^{35}P are 1.39 and 2.62 MeV respectively. Thus, the ground-state wave functions are dominated by configurations with the maximum allowed number of particles in the $2s_{1/2}$ orbit. Particularly, for ^{36}S the $(2s_{1/2})^4$ configuration represents 89% of the wave function. When the neutrons begin to fill the pf shell, the two orbitals become more and more degenerate (see Table I) inducing strong mixing in the wave functions. A valence space with degenerate $1d_{3/2}$ and $2s_{1/2}$ orbitals has the geometry of pseudo-SU(3), and maximal quadrupole coherence is obtained for two protons, i.e, for the sulphur isotopes. For three protons the quadrupole moment is strictly zero and beyond it changes sign leading to oblate shapes. Thus, we expect other nuclei as, for instance, the Ar isotopes to have small collectivity.

Notice, however, that strict degeneration is achieved only at $N=28$, where the neutron collectivity is rather small. In other words, there is a mismatch between the region where protons have collective wave functions ($N=28$) and the region were neutrons have quadrupole collectivity, that prevents the existence of a larger region of deformation. A compromise seems to take place for $Z=16$ and $N=26$ (^{42}S) or $N=24$ (^{40}S).

IV. SUMMARY

In this work we have studied the $N=28$ region far from the stability. We have built an effective interaction for sd active protons and pf active neutrons that is a natural generalization of successful sd-only and pf-only interactions. The agreement of the theoretical results and the experimental data is very satisfactory. However, much more experimental information is needed to obtain a complete understanding of the region. Accurate information on the 2^+ excitation energies, on the evolution of the $3/2^+$,$1/2^+$ doublet along the Cl and P chains, the single particle spectrum of ^{35}Si are challenges for the physics of exotic nuclei. We have also addressed the question of the magicity of $N=28$. A detailed analysis of the S_{2n}, 2^+ energies and occupation numbers allow us to conclude that magicity persists in the very neutron-rich regime, contrary to what happens at $N=20$. Finally our results show that the ^{40,42}S isotopes are well deformed, but the effect seems to be local; no large region of deformation is therefore expected.

Note added. The properties of several very neutron rich isotopes of Ar and S have recently been measured at the National Superconducting Cyclotron Laboratory at Michigan State University [31]. There is good agreement among our predictions and the new experimental results except for the $B(E2)$ of ^{46}Ar. The new 2^+ energies are displayed in Table I with an asterisk, whilst the corresponding $B(E2;2_1^+ \rightarrow 0_{\rm gs}^+)$ are shown in the table below.

		^{44}Ar	^{46}Ar	^{38}S	^{40}S	^{42}S
$B(E2)(e^2\text{fm}^4)$	Th	69	91	44	78	93
	Exp	69(8)	39(8)	47(6)	67(7)	79(12)

The predicted deformation parameters for ^{40,42}S are very similar to those extracted from the experimental $B(E2)$: 0.29 and 0.32 compared to 0.28 and 0.30.

ACKNOWLEDGMENTS

We want to thank A. Zuker for his decisive help in the determination of the effective interaction and G. Walter for enlightening discussions. This work has been partially supported by the IN2P3(France)-CICyT(Spain) agreements and by DGICyT (Spain) Grant No. PB93-263.

[1] C. Thibault *et al.*, Phys. Rev. C **12**, 193 (1975).
[2] C. Detraz, D. Guillemaud, G. Huber, R. Klapisch, M. Langevin, F. Naulin, C. Thibault, L. C. Carraz, and F. Touchard, Phys. Rev. C **19**, 171 (1978).
[3] G. Huber, F. Touchard, S. Buttenbach, C. Thibault, R. Klapisch, H. T. Duong, S. Liberman, J. Pinard, J. L. Vialle, P. Juncar, and P. Jacquinot, Phys. Rev. C **18**, 2342 (1978).
[4] D. Guillemaud, C. Detraz, M. Langevin, F. Naulin, M. de Saint-Simon, C. Thibault, F. Touchard, and M. Epherre, Nucl. Phys. **A246**, 37 (1984).
[5] A. Poves and J. Retamosa, Phys. Lett. B **184**, 311 (1987); A. Poves and J. Retamosa, Nucl. Phys. **A571**, 221 (1994).
[6] E. K. Warburton, J. A. Becker, and B. A. Brown, Phys. Rev. C **41**, 1147 (1990).
[7] N. Fukunishi, T. Otsuka, and T. Sebe, Phys. Lett. B **296**, 279 (1992).
[8] X. Campi, H. Flocard, A. K. Kerman, and S. Koonin, Nucl. Phys. **A251**, 193 (1975).
[9] O. Sorlin *et al.*, Phys. Rev. C **47**, 2941 (1993); O. Sorlin *et al.*, Nucl. Phys. **A583**, 763 (1995).
[10] H. V. Klapdor, J. Metzinger, and T. Oda, At. Data Nucl. Data Tables **31**, 81 (1984).
[11] A. Staudt, E. Bender, K. Muto, and H. V. Klapdor, At. Data Nucl. Data Tables **44**, 1 (1990).
[12] P. Möller and J. R. Nix, At. Data Nucl. Data Tables **39**, 213 (1988).
[13] P. Möller and J. R. Nix, At. Data Nucl. Data Tables**59**, 185 (1995).
[14] J. M. Pearson, Y. A. Aboussir, A. K. Dutta, R. C. Navak, M. Farine, and F. Tondeur, Nucl. Phys. **A258**, 1 (1991).
[15] T. R. Werner, J. A. Sheikh, W. Nazarewicz, M. R. Strayer, A. S. Umar, and M. Misu, Phys. Lett. B **335**, 259 (1994).
[16] A. Abzouzi, E. Caurier, and A. Zuker, Phys. Rev. Lett. **66**, 1134 (1991).
[17] G. Walter, *Proceedings of the Workshop on Nuclear Structure of Light Nuclei Far From Stability: Experiment and Theory*, edited by G. Klotz (CRN, Obernai, 1990), p. 71.
[18] B. H. Wildenthal, Prog. Part. Nucl. Phys. **11**, 5 (1984).
[19] A. Poves and A. Zuker, Phys. Rep. **70**, 4 (1981).
[20] S. Kahana, H. C. Lee, and C. K. Scott, Phys. Rev. **180**, 956 (1969).
[21] A. P. Zuker (private communication).
[22] J. Duflo and A. P. Zuker, Phys. Rev. C **52**, R1 (1995).
[23] A. Pape and M. S. Antony, At. Data Nucl. Data Tables **39**, 201 (1988).
[24] E. Caurier, A. P. Zuker, A. Poves, and G. Martínez-Pinedo, Phys. Rev. C **50**, 225 (1994).
[25] E. Caurier, code ANTOINE, Strasbourg, 1989 (unpublished).
[26] R. R. Whitehead, in *Moments Methods in Many Fermion Systems*, edited by B. J. Dalton, S. M. Grimes, J. D. Vary, and S. A. Williams (Plenum, New York, 1980), p. 235.
[27] D. H. Wilkinson and B. E. F. Macefield, Nucl. Phys. **A232**, 58 (1974).
[28] *Table of Isotopes*, 7th ed., edited by C. M. Lederer and V. S. Shirley (Wiley, New York, 1978).
[29] G. Audi and A. H. Wapstra, Nucl. Phys. **A565**, 1 (1993).
[30] A. Zuker, J. Retamosa, A. Poves, and E. Caurier, Phys. Rev. C **52**, R1741 (1995).
[31] H. Scheit *et al.*, Phys. Rev. Lett. **77**, 3967 (1996).